

# Spatiotemporal Phase Unwrapping for Real-Time Phase-Contrast Flow MRI

Markus Untenberger,<sup>1\*</sup> Markus Hüllebrand,<sup>2</sup> Lennart Tautz,<sup>2</sup> Arun A. Joseph,<sup>1,3</sup> Dirk Voit,<sup>1</sup> K. Dietmar Merboldt,<sup>1</sup> and Jens Frahm<sup>1,3</sup>

**Purpose:** To develop and evaluate a practical phase unwrapping method for real-time phase-contrast flow MRI using temporal and spatial continuity.

**Methods:** Real-time phase-contrast MRI of through-plane flow was performed using highly undersampled radial FLASH with phase-sensitive reconstructions by regularized nonlinear inversion. Experiments involved flow in a phantom and the human aorta (10 healthy subjects) with and without phase wrapping for velocity encodings of 100 cm·s<sup>-1</sup> and 200 cm·s<sup>-1</sup>. Phase unwrapping was performed for each individual cardiac cycle and restricted to a region of interest automatically propagated to all time frames. The algorithm exploited temporal continuity in forward and backward direction for all pixels with a “continuous” representation of blood throughout the entire cardiac cycle (inner vessel lumen). Phase inconsistencies were corrected by a comparison with values from direct spatial neighbors. The latter approach was also applied to pixels exhibiting a discontinuous signal intensity time course due to movement-induced spatial displacements (peripheral vessel zone).

**Results:** Phantom and human flow MRI data were successfully unwrapped. When halving the velocity encoding, the velocity-to-noise ratio (VNR) increased by a factor of two.

**Conclusion:** The proposed phase unwrapping method for real-time flow MRI allows for measurements with reduced velocity encoding and increased VNR. **Magn Reson Med** 74:964–970, 2015. © 2014 Wiley Periodicals, Inc.

**Key words:** flow MRI; real-time MRI; velocity-encoded MRI; phase-contrast MRI; phase unwrapping

## INTRODUCTION

Phase wrapping in velocity-encoded phase-contrast MRI is a frequent phenomenon when using bipolar flow-encoding gradients for a field of view that is too small along the flow velocity (phase) direction. This particu-

larly applies to studies of the ascending and descending aorta in patients who present with high flow velocities due to a vascular stenosis or valve dysfunction. On the other hand, it has been shown previously that a small velocity encoding (VENC) value is advantageous, because it enhances the signal-to-noise ratio (SNR) in the respective phase dimension (1,2). In particular, halving the VENC increases the velocity-to-noise ratio (VNR) by a factor of 2. Moreover, the improved tolerance to phase wraps in a clinical scenario simplifies the practical choice of a VENC value and therefore may reduce total examination times by eliminating the need for repeated scans.

In this study, we present a simple and robust method for phase unwrapping that focuses on a (vascular) region-of-interest (ROI) and mainly exploits the phase continuity along the temporal dimension. The approach is therefore best suited for real-time phase-contrast flow MRI, which provides velocity-encoded phase maps at high temporal resolution and with true temporal continuity (i.e., without merging data from multiple cardiac cycles) (3,4). The underlying MRI sequence takes advantage of a recently developed real-time MRI technique (5,6) in which parallel image reconstruction from highly undersampled radial datasets is defined as the solution of a nonlinear inverse problem, which jointly estimates all coil sensitivities and the desired image (7). In addition, this optimization process is constrained by temporal regularization (5,8). The proposed phase unwrapping method is experimentally validated using phase-contrast flow MRI data of a phantom and the human aorta for a group of healthy young adults.

## THEORY

Figure 1 shows a flow chart of the proposed method, which comprises a preprocessing part and a main phase unwrapping part. In brief, manual selection of a single ROI (i.e., a vessel) is followed by an automatic propagation of contours across time frames. The actual phase unwrapping relies on an algorithm originally described by Itoh (9). Here, it is applied to each individual cardiac cycle along both directions of the time axis for all ROI pixels that exhibit a continuous signal intensity time course (i.e., primarily, pixels in the central area of the vessel lumen). Phase inconsistencies and subsequently also pixels with a discontinuous signal intensity time course (e.g., in the periphery of the vessel lumen) are corrected by a comparison with already corrected nearest spatial neighbors. The proposed method therefore follows previous ideas that combined temporal and spatial information to achieve robust phase unwrapping of

<sup>1</sup>Biomedizinische NMR Forschungs GmbH am Max-Planck Institut für biophysikalische Chemie, Göttingen, Germany.

<sup>2</sup>Fraunhofer MEVIS Institute for Medical Image Computing, Bremen, Germany.

<sup>3</sup>German Center for Cardiovascular Research (DZHK), Göttingen, Germany. Grant sponsors: German Centre for Cardiovascular Research (DZHK), German Ministry of Education and Research (BMBF), and the Max-Planck-Gesellschaft and Fraunhofer Gesellschaft.

\*Correspondence to: Markus Untenberger, Biomedizinische NMR Forschungs GmbH am Max-Planck-Institut für biophysikalische Chemie, 37070 Göttingen, Germany. E-mail: muntenb@mpibpc.mpg.de

Received 19 June 2014; revised 29 August 2014; accepted 1 September 2014

DOI 10.1002/mrm.25471

Published online 10 October 2014 in Wiley Online Library (wileyonlinelibrary.com).

© 2014 Wiley Periodicals, Inc.

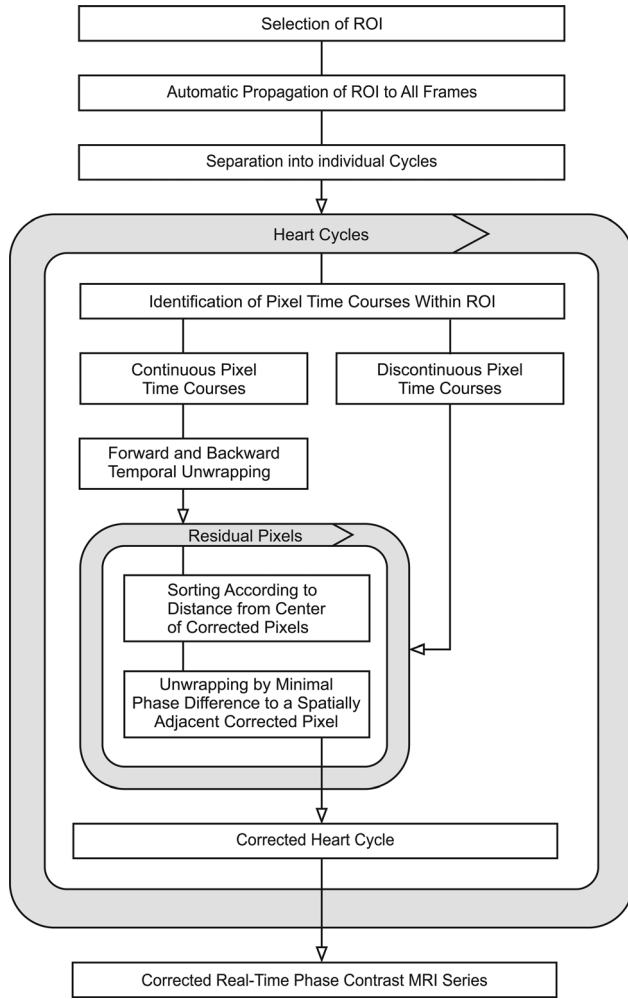


FIG. 1. Schematic outline of the algorithm proposed for phase unwrapping of real-time phase-contrast flow MRI data.

velocity-encoded MRI signals in the presence of vascular movements [in particular, see Yang et al. (10) and Salfity et al. (11)].

#### Automatic Region Propagation

Preprocessing of real-time MRI data starts with the manual definition of a ROI in a single diastolic magnitude image as depicted in Figure 2 (top row, left-most image). In this example, the ROI covers the ascending aorta with phase wraps during systole (Fig. 2, second row). Its contours are automatically propagated to all magnitude images and phase-contrast maps (Fig. 2, third row). The underlying method is part of the CAIPI (Integrated Processing of Multimodal Cardiac Image Data) prototype software for the analysis of cardiovascular image data (Fraunhofer MEVIS, Bremen, Germany) and has been described in detail previously (12,13). Briefly, in order to transfer the delineation of the ROI to the entire series of real-time images, the vessel motion is estimated using the Morphon approach, a phase-based registration method (13). The calculated motion is used to propagate the vessel boundaries from the reference frame through the image series. This process is implemented as a two-

step approach to minimize error propagation. First, the image series is split into individual heart cycles. Starting from the reference frame, in which the contour was drawn, corresponding time frames in other heart cycles are identified in accordance to the detected contraction phase. The Morphon approach is applied to compensate for spatial displacements due to breathing between these time frames. This nonrigid registration method estimates the deformation between two frames from the phase difference between quadrature filter responses, which are intensity-invariant and proportional to the spatial change. This calculation is iterated in a scale space to handle both noise and motion in different orders of magnitude. In a second step, the contours of these reference frames are propagated through each cardiac cycle using serial deformation fields calculated with the same method.

#### Phase Unwrapping

After propagation of the ROI and automatic separation of a real-time MRI series into successive cardiac cycles for individual analyses, a first step refers to the identification of pixels with a continuous signal intensity time course within the previously defined ROIs yielding binary masks  $R_1, \dots, R_N$ . Continuous pixels  $x$  are shared by all  $N$  ROIs and formally defined as

$$\{x : x \in \bigcap_{i=1}^N R_i\}. \quad [1]$$

They represent blood signal throughout the entire cardiac cycle and mainly refer to the inner area of a vessel which may be spatially displaced due to cardiac

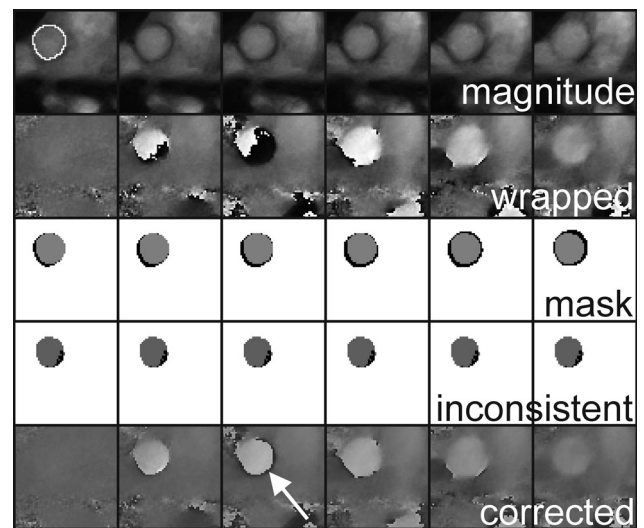


FIG. 2. Real-time phase-contrast flow MRI of the human aorta at  $VENC = 100 \text{ cm} \cdot \text{s}^{-1}$  (simulated). First row: magnitude images with ROI. Second row: phase-contrast maps with phase wraps. Third row: masks obtained for pixels with a continuous (gray) and discontinuous (black) signal intensity time course. Fourth row: continuous pixels with consistent (gray) and inconsistent (black) forward and backward phase unwrapping. Fifth row: phase-contrast maps after correction. Residual pixels (white arrow) lie outside the analyzed ROI and most likely refer to the vessel wall.

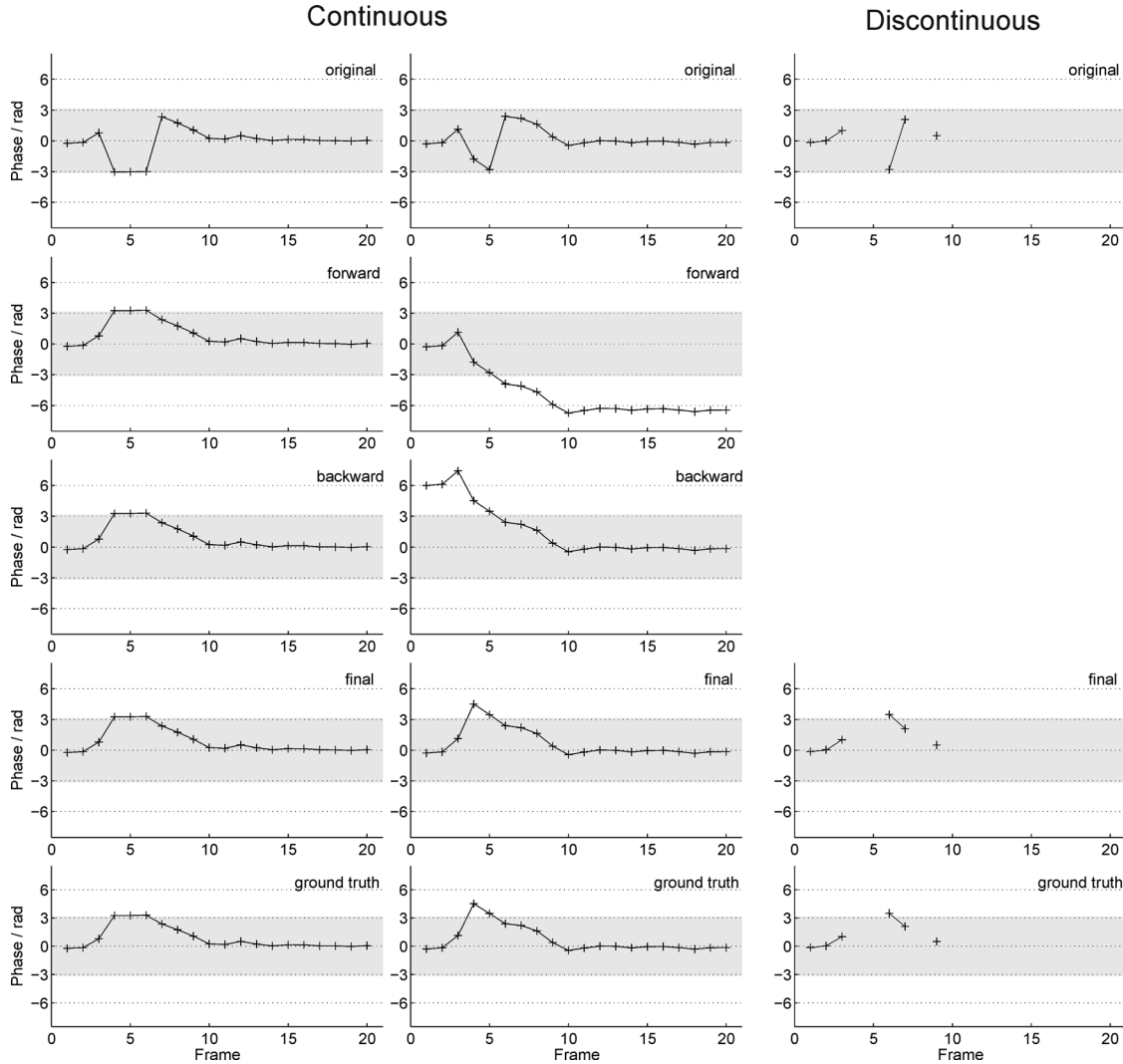


FIG. 3. Phase unwrapping for three different types of single pixels and real-time phase-contrast flow MRI of the human aorta (single cardiac cycle) at  $\text{VENC} = 100 \text{ cm}\cdot\text{s}^{-1}$  (simulated). Time courses are shown for continuous signal intensity with (left) and without (middle) identical phase values for forward and backward unwrapping and discontinuous signal intensity (right). Top to bottom: The individual traces correspond to the artificially wrapped time courses, forward and backward phase unwrapping with the method described by Itoh (9) (continuous time courses only), corrected time courses after adding spatial continuity (if applicable), and ground truth obtained for  $\text{VENC} = 200 \text{ cm}\cdot\text{s}^{-1}$ .

movements or free breathing. Accordingly, pixels in the outer zones of each ROI eventually exhibit a discontinuous signal intensity time course, in the sense that they represent aortic blood during one part of the cardiac cycle and surrounding tissue outside the aorta at other times. Thus, discontinuous pixels  $y$  defined as

$$\{y : y \in R_i, i \in \{1, \dots, N\} \wedge y \notin \bigcap_{i=1}^N R_i\} \quad [2]$$

fall within some ROIs but lie outside others. The third row in Figure 2 depicts the binary masks obtained for continuous (gray) and discontinuous pixels (black).

Continuous time series are unwrapped by a pixel-wise application of Itoh's method: First in a forward direction, then backward with reverse temporal ordering. Itoh's method relies on the initial identification of a time point with correct phase value (i.e. without phase wrapping).

This condition is fulfilled easily, as many phases during a cardiac cycle exhibit only low flow velocities. First, respective diastolic frames are identified using the coregistered electrocardiographic (ECG) time stamp (e.g., Fig. 2, second row, left-most image). Second, the phase difference between the initial time point and the next time point is calculated and added to the initial phase. This step is repeated with the newly unwrapped time point as the initial value until the end of the time course or path is reached. If the initial pixel has a correct phase and if all phase differences are between  $-\pi$  and  $\pi$ , then all phases will be unwrapped correctly. In fact, this latter condition is fulfilled if the phase values obtained by forward and backward propagation agree. An example is shown in Figure 3 (left column) for a real-time MRI study of the human aorta. Phase wrapping at  $\text{VENC} = 100 \text{ cm}\cdot\text{s}^{-1}$  was simulated using data of an acquisition at  $\text{VENC} = 200 \text{ cm}\cdot\text{s}^{-1}$ , which served as ground truth.

Residual pixels with continuous time courses but temporally inconsistent phase values are sorted according to their distance from the center of gravity of already corrected pixels. Starting with the most central uncorrected pixel, the phase differences with its already corrected nearest neighbors (maximum of four) are calculated. Unwrapping is then performed by adding the minimum phase difference to the initial value (Fig. 3, middle column). This approach ensures—and inherently assumes—a very local (i.e., pixel-wise) smoothness or spatial continuity of the phase (i.e., flow) within a vessel, while moving from inner corrected pixels to outer still uncorrected pixels. Subsequently, the same strategy is applied to all pixels with a discontinuous time course, again by pursuing a circular growth from the inner zone of pixels with reliable phase unwrapping to the periphery of the vessel lumen. The entire procedure is outlined in Figure 3, which depicts the treatment of two continuous signal intensity time courses with and without identical phases during forward and backward treatment (left and middle column, respectively) as well as a discontinuous time course (right column).

## METHODS

### Real-Time Phase-Contrast Flow MRI

All studies were performed on a clinical 3T MRI system (Tim Trio, Siemens Healthcare, Erlangen, Germany) using a cardiac coil with 16 anterior and 16 posterior elements. Flow evaluations in real time were accomplished with the use of a highly undersampled radial FLASH sequence with image reconstruction by regularized nonlinear inversion (4,5). The nonlinear inversion method was modified for phase-contrast flow MRI to yield phase-sensitive reconstructions of two series of differently flow-encoded images, whereas phase-contrast maps were obtained without any temporal filter (3,4,6). Magnitude images and phase-contrast maps were computed online using a server with  $2 \times 4$  graphics processing units (sysGen/TYAN Octuple-GPU, 2x Intel Westmere E5620 processor, 48GB RAM, Sysgen, Bremen, Germany) which was fully integrated into the reconstruction pipeline of the commercial MRI system (8,14).

For both phantom and human studies two sequential images with and without a bipolar flow-encoding gradient were obtained from only 7 spokes within an acquisition time of slightly above 20 ms each (4). In order to allow for a proper VNR analysis, the measurements with  $\text{VENC} = 200 \text{ cm}\cdot\text{s}^{-1}$  were performed with the same temporal resolution of 43.4 ms as required for  $\text{VENC} = 100 \text{ cm}\cdot\text{s}^{-1}$ . The experimental parameters for real-time phase-contrast flow MRI were: repetition time  $\text{TR} = 3.10 \text{ ms}$ , echo time  $\text{TE} = 2.21 \text{ ms}$ , flip angle  $10^\circ$ , nominal in-plane resolution  $1.3 \times 1.3 \text{ mm}^2$ , and slice thickness 6 mm. Dynamic reconstructions of phase-contrast maps therefore correspond to a rate of 23 frames per second.

The algorithm for phase unwrapping was developed in MATLAB (MathWorks, Natick, Massachusetts, USA) and a respective off-line implementation was applied for analyzing the data of the present study.

### Phantom Studies

The flow phantom was made of acrylic glass and filled with stationary water. It comprised two tubes (i.e., 10 and 20 mm diameter) performing a U turn in a coronal plane that resulted in four areas of through-plane flow (two tubes, two directions). The tubes were connected outside the phantom, and flow was driven by a computer-controlled immersion pump (Lux Plus KTW270, Herzog, Göttingen, Germany). Pulsatile flow as in the human aorta was generated by a repetitive pump protocol with a brief period (0.4 s) of high velocity followed by a longer period (1.6 s) of lower velocity (repetition cycle, 2.0 s). High- and low-flow conditions referred to pump voltages differing by a factor two (15). During high-flow conditions, phase wraps occurred for  $\text{VENC} = 100 \text{ cm}\cdot\text{s}^{-1}$  but not for  $\text{VENC} = 200 \text{ cm}\cdot\text{s}^{-1}$ .

### Human Studies

Ten young volunteers without known illness and contraindications for MRI participated in the study. The study received Institutional Review Board approval and written informed consent was obtained from each subject before MRI. Blood flow was measured during free breathing and simultaneously in the ascending and descending aorta using a single plane perpendicular to the ascending aorta at the level of the right pulmonary artery. For each volunteer real-time phase-contrast flow MRI was performed with  $\text{VENC} = 100 \text{ cm}\cdot\text{s}^{-1}$  (three measurements) and  $\text{VENC} = 200 \text{ cm}\cdot\text{s}^{-1}$  (one measurement). Depending on where a phase wrap occurred, either the ascending or descending aorta was unwrapped and analyzed.

### Simulated Data

Simulations were performed using human flow MRI data with  $\text{VENC} = 200 \text{ cm}\cdot\text{s}^{-1}$  and no phase wraps. Simulated phase wraps were generated by retrospectively reducing the phase interval from  $(-\pi, \pi)$  to  $(-\pi/2, \pi/2)$ . Values above  $\pi/2$  (below  $-\pi/2$ ) were added (subtracted) by  $\pi$ , while all values within  $(-\pi/2, \pi/2)$  remained unchanged. To obtain wrapped phase data within  $(-\pi, \pi)$ , all values were subsequently multiplied by two. The corresponding artificial  $\text{VENC} = 100 \text{ cm}\cdot\text{s}^{-1}$  data sets were unwrapped and analyzed in the same way as for the true  $\text{VENC} = 100 \text{ cm}\cdot\text{s}^{-1}$  phantom and human data, and the results were compared with the evaluations of the original  $\text{VENC} = 200 \text{ cm}\cdot\text{s}^{-1}$  data without phase wraps (ground truth).

### Velocity-to-Noise Ratio

For each time frame, the phase-contrast flow MRI reconstruction yields two differently flow-encoded sets of  $c = (1, \dots, M)$  complex images  $q_{1,c}$  and  $q_{2,c}$ , where  $M$  denotes the number of MRI receive channels. These sets of images are combined into a single complex phase-contrast map

$$q_{pc} = \sum_{c=1}^M q_{c,1} \bar{q}_{c,2}, \quad [3]$$

where the bar represents the complex conjugate. The phase of  $q_{pc}$  is converted into a velocity map. The VNR is calculated according to

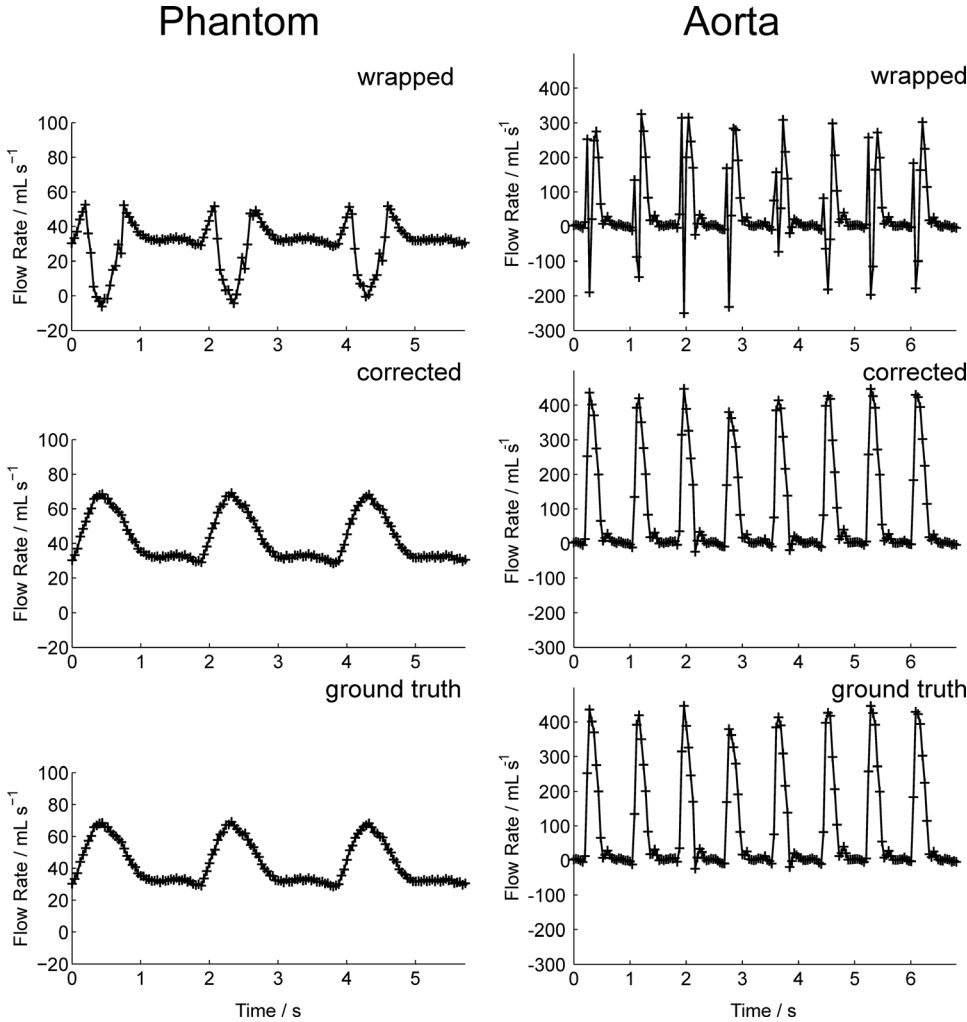


FIG. 4. Real-time flow rates for a flow phantom and the ascending aorta (single subject). Top: simulated phase-wrapped flow MRI data at  $VENC = 100 \text{ cm}\cdot\text{s}^{-1}$ . Middle: corrected data after phase unwrapping. Bottom: ground truth for  $VENC = 200 \text{ cm}\cdot\text{s}^{-1}$ .

$$VNR = \frac{|v|\pi}{VENC} SNR, \quad [4]$$

where  $|v|$  is the mean value of the absolute velocity in an ROI and the SNR is taken from the magnitude images of  $Q_{pc}$  (1,2).

Possible VNR improvements were evaluated in the phantom and all subjects using single frames with high velocity in the selected ROI. In human subjects, these frames referred to peak systole. The SNR of the magnitude image was determined by segmenting the whole image using the method of Otsu (16) into a foreground and background signal. The SNR was then calculated by dividing the mean of the foreground by the standard deviation of the background signal.

## RESULTS

The proposed method for phase unwrapping of real-time phase-contrast flow MRI data resulted in a robust correction of velocity-encoded phase values both in vitro and in vivo. The reliability of the approach was first validated using simulated data of a flow phantom and the human aorta as shown in Figure 4, where phase wraps occur for flow velocities larger than  $100 \text{ cm}\cdot\text{s}^{-1}$ . The

traces show the mean flow rates averaged across the vessel lumen for the artificially wrapped and corrected data in comparison to ground truth. Without correction, the affected flow rates (i.e., flow volumes per unit time) are reduced, whereas phase unwrapping restores correct velocities (data not shown) and flow rates.

Complementing the results for single-pixel phase values (velocities) in Figure 3, the time frames shown in the bottom row of Figure 2 depict corrected phase-contrast maps for the human aorta at  $100 \text{ cm}\cdot\text{s}^{-1}$  (simulated). In all cases, i.e. in all pixels of the propagated ROIs, phase unwrapping exactly restored the phase values of the original acquisition at  $VENC = 200 \text{ cm}\cdot\text{s}^{-1}$  (ground truth). Residual pixels (bottom row of Fig. 2, white arrow) were found outside the analyzed ROI and most likely refer to the vessel wall.

Figure 5 demonstrates the reliable performance of the phase unwrapping method for prospectively acquired real-time phase-contrast flow MRI data at  $VENC = 100 \text{ cm}\cdot\text{s}^{-1}$ . The example again depicts corrected flow rates for a phantom and the human aorta. The mean peak flow velocities averaged across cardiac cycles for acquisitions without phase wraps ( $VENC = 200 \text{ cm}\cdot\text{s}^{-1}$ ) and after phase unwrapping ( $VENC = 100 \text{ cm}\cdot\text{s}^{-1}$ ) are summarized in Table 1 for all subjects together with the

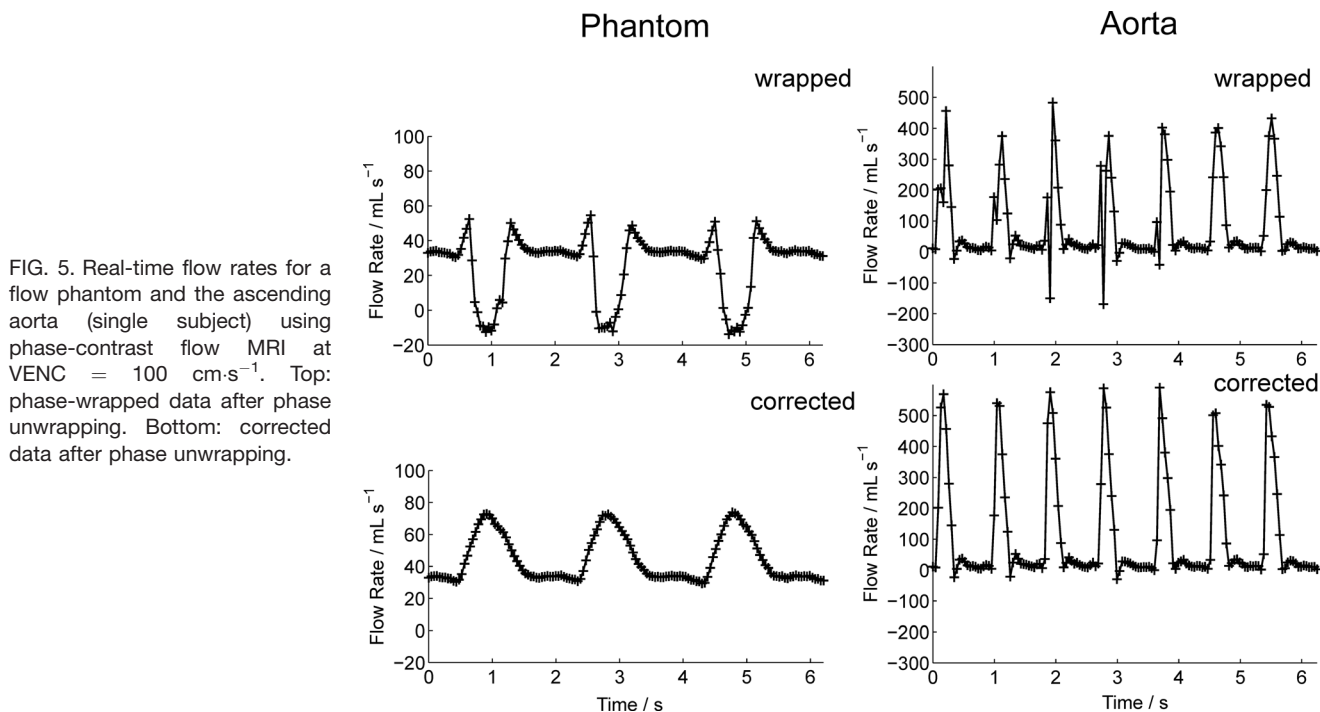


FIG. 5. Real-time flow rates for a flow phantom and the ascending aorta (single subject) using phase-contrast flow MRI at  $VENC = 100 \text{ cm}\cdot\text{s}^{-1}$ . Top: phase-wrapped data after phase unwrapping. Bottom: corrected data after phase unwrapping.

corresponding VNR values. Peak velocities and their standard deviations reflect intersubject differences as well as intrasubject variability between two independent measurements and 15–20 cardiac cycles. The VNR improvement was about the expected value of two for a halved  $VENC$  value in almost all cases. Variations in individual subjects are due to variations in SNR of the magnitude images and mean velocities within the ROI. Across subjects, the mean VNR values  $\pm$  standard deviation were  $7.0 \pm 4.0$  for  $VENC = 200 \text{ cm}\cdot\text{s}^{-1}$  (no phase wraps) and  $16.9 \pm 6.0$  for  $VENC = 100 \text{ cm}\cdot\text{s}^{-1}$  (after phase unwrapping).

## DISCUSSION

This study describes a simple and robust approach to phase unwrapping of real-time phase-contrast flow MRI data that expands upon the method of Itoh (9) by

exploiting temporal and spatial continuity. Previously, a method for temporal phase unwrapping, which treats all pixel intensity time courses as continuous and only uses forward unwrapping, has been applied to ECG-gated cine flow MRI data (17). This strategy ignores discontinuous pixel contributions due to motion of the aorta, which seems to be acceptable for the analysis of a single time-averaged cine MRI data set from multiple cardiac cycles. However, in order to benefit from real-time MRI advantages such as free breathing and functional access to individual cardiac cycles, a more elaborate multistep method for phase unwrapping is required that includes a treatment of pixels with discontinuous signal intensity time courses. On the other hand, the present method is less demanding than a previously described method for spatiotemporal phase unwrapping that attempts to track the exact path of pixel intensities throughout all frames of a cardiac cycle (10). Provided the vascular ROI as a

Table 1  
Peak Flow Velocity and VNR for Real-Time Flow MRI

| Subject | $VENC = 200 \text{ cm}\cdot\text{s}^{-1}$ without phase wraps |                | $VENC = 100 \text{ cm}\cdot\text{s}^{-1}$ after phase unwrapping |                |
|---------|---|----------------|--|----------------|
|         | Peak velocity, $\text{cm}\cdot\text{s}^{-1}$                  | VNR            | Peak velocity, $\text{cm}\cdot\text{s}^{-1}$                     | VNR            |
| Phantom | $121.2 \pm 1.8$   | $15.0 \pm 1.5$ | $123.8 \pm 2.1$  | $26.8 \pm 2.5$ |
| 1       | $75.5 \pm 6.6$  | $8.7 \pm 1.4$  | $81.2 \pm 8.4$   | $17.7 \pm 2.4$ |
| 2       | $-85.3 \pm 3.8$   | $6.2 \pm 2.7$  | $-98.1 \pm 4.1$  | $14.8 \pm 7.6$ |
| 3       | $91.9 \pm 11.8$   | $5.6 \pm 0.6$  | $94.5 \pm 21.4$  | $10.8 \pm 2.1$ |
| 4       | $-90.5 \pm 6.2$   | $4.4 \pm 1.8$  | $-101.2 \pm 5.6$   | $13.4 \pm 4.2$ |
| 5       | $94.2 \pm 7.7$  | $6.0 \pm 1.2$  | $124.8 \pm 22.6$   | $13.1 \pm 1.8$ |
| 6       | $-104.3 \pm 7.5$  | $5.5 \pm 1.9$  | $-94.1 \pm 7.2$  | $11.7 \pm 3.9$ |
| 7       | $-109.0 \pm 8.2$  | $7.3 \pm 1.4$  | $-109.7 \pm 6.3$   | $17.6 \pm 2.4$ |
| 8       | $97.9 \pm 10.0$   | $11.6 \pm 1.8$ | $110.0 \pm 11.2$   | $29.7 \pm 3.1$ |
| 9       | $122.8 \pm 7.4$   | $14.6 \pm 1.2$ | $112.9 \pm 20.7$   | $24.9 \pm 2.6$ |
| 10      | $102.1 \pm 17.9$  | $7.4 \pm 2.0$  | $110.5 \pm 27.3$   | $15.2 \pm 4.1$ |

Data are presented as the mean  $\pm$  standard deviation of 15–20 cardiac cycles. Peak velocities refer to either the ascending or descending aorta (negative values) depending on the occurrence of phase wraps at  $VENC = 100 \text{ cm}\cdot\text{s}^{-1}$ .

whole is reliably propagated to cope with movement-related displacements, such a complex task is indeed not necessary, as quantitative flow parameters are obtained by integrating phase values across the entire vessel lumen.

A known limitation of the basic Itoh algorithm is the higher-order phase wraps if the absolute phase difference between two adjacent time points is equal to or larger than  $\pi$  (9). In addition, problems may occur for phase wraps in two or three dimensions, which increase the degree of complexity as well as the corresponding computational demand [e.g., see (18–21)]. It remains to be seen whether these methods may be adapted to unwrap real-time phase-contrast flow MRI data. In general, the need for a phase correction, which is caused by a VENC value that is too low, should not be confused with the occurrence of phase wraps, which are due to the presence of turbulence or other complex flow patterns (e.g., in patients with stenosis or valve dysfunction). In these cases, phase errors are due to contributions from higher-order through-plane flow (e.g., accelerated flow or jerk) or in-plane flow components, which should not be translated into false through-plane velocities by phase unwrapping. Instead, it seems mandatory to minimize respective phase contributions by adding motion-compensating magnetic field gradients to the phase-contrast MRI acquisition technique rather than to seek a correction.

The computation time for the present phase unwrapping method, which was implemented in MATLAB and applied off-line, was about 10–15 s for a typical real-time phase-contrast MRI data set of 370 frames. This duration can be reduced further by parallelizing the algorithm (e.g., for multiple cardiac cycles) and by porting the code into a faster programming language such as C/C++. In addition, the current workflow for phase unwrapping is tedious due to the sequential application of two different software packages for segmentation/propagation and phase unwrapping, respectively. However, the currently prepared integration of the phase unwrapping algorithm into the CAIPI software will provide an easy-to-use tool for an almost completely automatic analysis of real-time phase-contrast maps with low VENC values and high VNR based on reliable phase unwrapping. This integration will facilitate more extended clinical trials of large patient cohorts.

In conclusion, the proposed phase unwrapping method for real-time flow MRI allows for measurements with reduced velocity encoding and increased VNR. By treating individual cardiac cycles with temporal forward and backward unwrapping and by identifying pixels with and without continuous support representing the same tissue throughout the cardiac cycle, the method exploits the true temporal continuity of a real-time MRI

acquisition and offers robust performance for moving vessels.

## REFERENCES

- Centuro TE, Smith GD. Signal-to-noise in phase angle reconstruction: dynamic range extension using phase reference offsets. *Magn Reson Med* 1990;15:420–437.
- Pelc NJ, Herfkens RJ, Shimakawa A, Enzmann DR. Phase contrast cine magnetic resonance imaging. *Magn Reson Q* 1991;7:229–254.
- Joseph AA, Merboldt KD, Voit D, Zhang S, Uecker M, Lotz J, Frahm J. Real-time phase-contrast MRI of cardiovascular blood flow using undersampled radial fast low-angle shot and nonlinear inverse reconstruction. *NMR Biomed* 2012;25:917–924.
- Joseph AA, Kowallick JT, Merboldt KD, Voit D, Schätz S, Zhang S, Sohns JM, Lotz J, Frahm J. Real-time flow MRI of the aorta at a resolution of 40 ms. *J Magn Reson Imaging* 2014;40:206–213.
- Uecker M, Zhang S, Voit D, Karaus A, Merboldt KD, Frahm J. Real-time MRI at a resolution of 20 ms. *NMR Biomed* 2010;23:986–994.
- Frahm J, Schätz S, Untenberger M, Zhang S, Voit D, Merboldt KD, Sohns JM, Lotz J, Uecker M. On the temporal fidelity of nonlinear inverse reconstructions for real-time MRI—the motion challenge. *Open Med Imaging J* 2014;8:1–7.
- Uecker M, Hohage T, Block KT, Frahm J. Image reconstruction by regularized nonlinear inversion—joint estimation of coil sensitivities and image content. *Magn Reson Med* 2008;60:674–682.
- Uecker M, Zhang S, Voit D, Merboldt KD, Frahm J. Real-time MRI—recent advances using radial FLASH. *Imaging Med* 2012;4:461–476.
- Itoh K. Analysis of the phase unwrapping algorithm. *Appl Opt, OSA* 1982;21:2470–2470.
- Yang GZ, Burger P, Kilner PJ, Karwatowski SP, Firmin DN. Dynamic range extension of cine velocity measurements using motion registered spatiotemporal phase unwrapping. *J Magn Reson Imaging* 1996; 6:495–502.
- Salfity MF, Huntley JM, Graves MJ, Marklund O, Cusack R, Beauregard DA. Extending the dynamic range of phase contrast magnetic resonance velocity imaging using advanced higher-dimensional phase unwrapping algorithms. *J R Soc Interface* 2006;3:415–427.
- Hüllebrand M, Hennemuth A, Messroghli D, Kühne T. An OsiriX plugin for integrated cardiac image processing research. *Proc SPIE Med Imaging* 2014;9039:90390D–7.
- Tautz L, Hennemuth A, Peitgen HO. Motion analysis with quadrature filter based registration of tagged MRI sequences. In: Camara O, Mansi T, Pop M, Rhode K, Sermesant M, Young A, editors. *Statistical atlases and computational models of the heart. Imaging and modeling challenges*. Berlin, Heidelberg: Springer; 2011. p 257–266.
- Schätz S, Uecker M. A multi-GPU programming library for real-time applications. In: *Algorithms and architectures for parallel processing*. *Lect Notes Comp Sci* 2012;7439:114–128.
- Joseph AA, Voit D, Schätz S, Merboldt KD, Frahm J. Towards Real-Time 3D Phase-Contrast Flow MRI. In *Proceedings of the 21st Annual Meeting of ISMRM, Salt Lake City, Utah, USA, 2013*. p. 4567.
- Otsu N. A threshold selection method from gray-level histograms. *IEEE T Syst Man Cyb* 1979;9:62–66.
- Xiang QS. Temporal phase unwrapping for CINE velocity imaging. *J Magn Reson Imaging* 1995;5:529–534.
- Ghiglia DC, Pitt MD. *Two-dimensional phase unwrapping: theory, algorithms and software*. New York: John Wiley & Sons; 1998.
- Tomioka S, Nishiyama S. Phase unwrapping for noisy phase map using localized compensator. *Appl Opt* 2012;51:4984–4994.
- Huntley JM. Three-dimensional noise-immune phase unwrapping algorithm. *Appl Opt* 2001;40:3901–3908.
- Liu W, Tang X, Ma Y, Gao J. 3D phase unwrapping using global expected phase as a reference: application to MRI global shimming. *Magn Reson Med* 2013;70:160–168.